Journal of Engineering and Applied Sciences 12 (Special Issue 6): 7951-7958, 2017
ISSN: 1816-949X

Prediction of MAF Parameters for AISI 316 SS using RBFNN and ANN Based Box-Behnken Design

Saad Hameed Al-Shafaie
Department of Metallurgical Engineering, College of Materials Engineering,
Babylon University, Hillah, Iraq

Abstract: This study represents work suggestion an ideological technique to solve optimization problem with multi-response enclosing Magnetic Abrasive Finishing (MAF) of stainless steel 316 (AISI 316 SS) using Artificial Neural Network (ANN) and Radial Basics Function Neural Network (RBFNN) methods based on Box Behnken design. The prediction of MAF is done by choosing input process parameters such as number of cycles of pole geometry, cutting velocity, amplitude of pole geometry, current, working gap and finishing time, whereas the output responses were Metal Removal Rate (MRR) and Surface Roughness (SR). Each node achieves an easy process in calculating its response from its independent variable that is conveyed through links joined to another. It is concluded that the error obtained in RBFNN Model is bigger than that ANN Model. In the end, it was proved that the create network's model was built using ANN tool that gives the predicted result when compared to the RBFNN Model.

Key words: Magnetic abrasive finishing, metal removal rate, neural network, box behnken design, radial basics function neural networks, surface roughness

INTRODUCTION

Finishing is a kind of machining processes for extremely raising the surface quality of a machined object when maintaining stable precision and enhancing the machining accuracy grade (Bang-Zhong and Jin-Jin, 2005). The surface finish has a pivotal effect on important functional characteristics like power losses and wear resistance because the friction on the engineering components (Jayakumar, 2001). Abrasive finishing can be divided into two types of technologies. One is traditional methods and other is advanced methods of finishing process. In the manufacturing of precision parts, the traditional methods such as honing, lapping, grinding, etc., are labour intensive, comparatively less controllable for finishing operations. These operations usually use a rigid tool that undergoes the Workpiece (WP) to essential stresses which may cause some defects resulting in decreased reliability and strength of the WP Considerable advanced fine finishing operations have been improved to precisely control the abrading forces, one of these processes is the Magnetic Abrasive Finishing (MAF) (Singh *et al*., 2010). This process removes an amount of material by the rotation and indentation of magnetic abrasive particles in the circular tracks.

The specialty of MAF process was capability to control the flexibility of the tool, ferromagnetic powder sealing by a magnetic field, one can control the density and rigidity of the magnetic brush that help to change the topography of magnetic flux in the working gap. Yamaguchi and Shinmura (1999) have examined the microscopic changes in the surface texture of SUS304 stainless steel disk resulting from an internal magnetic abrasive finishing process using sintered magnetic abrasive powder of a ferromagnetic substance (Fe_2O_3) and pure aluminum. Yamaguchi and Shinmura (2000) have proposed an internal magnetic abrasive finishing process using a pole rotation system to produce highly finished inner surfaces of SUS304 stainless steel tubes. MAF setup has designed and fabricated by Jain *et al*. (2001). The performance of the setup has also studied on non-magnetic stainless steel with the use of loosely bounded MAPs (Mechanical mixing of ferromagnetic Powder and Abrasive powder with a small amount of lubricant). It concluded that working gap and circumferential speed of the workpiece are the parameters which significantly influence the material removal, change in surface Roughness value (Ra). The effectiveness and validity of a MAF method to refine rough surfaces and sharp edges of silver steel bars have investigated by Khairy (2001), using a sintered mixture of Al_2O_3 and iron powder. Chang *et al*. (2002) have described the process principle and the finishing characteristics of a mechanical mixture of SiC abrasive and ferro magnetic particles with a SAE30 lubricant as unbounded magnetic

abrasive within cylindrical magnetic abrasive finishing. Raghuram and Joshi (2008). Have proposed analytical model for the surface roughness in polishing stainless steel work surface. The model found to agree reasonably well with the experimental results. Kwak and Shin (2011) improved the magnetic force for MAF of AZ31B magnesium alloy. The result indicated that the magnetic force intensity of magnetic table and spindle speed of inductor was significant parameters for improvement of surface roughness in the second-generation MAF process. This study illustrates work suggestion, an intellectual approach in solving multi-response optimization problem involving MAF of AISI 316 SS using Radial Basics Function Neural Network (RBFNN) and Artificial Neural Network (ANN) techniques and compare between them.

MATERIALS AND METHODS

An electromagnetic inductor has designed and manufactured using for finishing flat surfaces WP by a vertical milling machine. The inductor was a steel rod wrapped around a coil of wires, magnetic force was generated on the working gap between pole and WP, the gap was filled with powder and the current was applied by (DC) power supply. The abrasive powder used 400 μm mesh size, contain 67% Fe_2O_3 and 33% industrial diamond. The work piece plate material is AISI 316 SS with chemical composition listed in Table 1. After MAF operation, the following techniques were utilized to measure the MRR and SR of the machining specimens:

- Digital weight balance (Denver instrument) with an accuracy of 0.01 mg to decide the MRR by measuring the weight difference (ΔW) of the workpiece
- Surface Roughness tester (TR220) to measure the surface roughness before and after the MAF process (ΔRa)
- Scanning Electron Microscopy (SEM) (Model; Inspect S50) to conduct surface topology observations

The process parameters in this investigation are number of cycles of pole geometry (A), cutting velocity (B), amplitude of pole geometry (C), current (D), working gap (E) and Finishing time (F) as illustrated in the Table 2 whereas MRR with SR were used as the response for AISI 316 SS. Six process parameters with three levels totally of 54 tests were carried out according to Box-Behnken approach as shown in the Table 3.

Table 1: Chemical composition of AISI 316 SS

Elements	Weight (%)
C	0.080
Mn	2.000
Si	0.750
P	0.045
S	0.030
Cr	18.000
Mo	3.000
Ni	14.000
N	0.100

Table 2: Process variables and their levels used in the experiment of AISI 316 SS

		Levels		
Input	Symbol	1	2	3
No. of cycles of pole geometry	A	2	6	10
Cutting velocity (rpm)	B	200	700	1200
Amplitude of pole geometry (mm)	C	6	12	18
Current (A)	D	2	4	6
Working gap (mm)	E	1	2	3
Finishing time (min)	F	12	16	20

Radial basics function neural networks: Three layers of RBFNN, input, out-put and the RBF (hidden) layer as in Fig. 1. RBFNN demand minimal computational time over back propagation because of the hidden to output layer are to be specified by the error signal values.

The hidden layer inputs consisting of the scalar weights of linear interactions genitive the vector inputs $X = (X_1, X_2, ..., X_n)^T$ where unity values are specified to the scalar weights. Subsequently, the total vector input builds up to every neuron in the hidden layer. The vector that comes in are mapped to the radial basis method in each hidden node. Vector $Y = (Y_1, Y_2, .., Y_n)$ supplied by the output layer for n outputs by the response's linear combination conformable to the hidden nodes in producing output that is final. Figure 1 illustrates the construction of a typical response RBFNN; the response of the network is obtained as:

$$y = f(x) = \sum_{i=1}^{k} w_i \varphi_i(x) \quad (1)$$

Where:

f(x) = The final response

φ_i = Performs the radial basis use of the ith hidden node

w_i = Perform the hidden into output weight with respect to the ith hidden node and hidden nodes in whole number is k

An RBF is a multi-dimensional function which explains the remoteness among a pre-defined centre vector and a given input vector. Different kinds of

Table 3: Process variables and their corresponding responses

Experiment No.	No. of cycles of pole geometry A	Cutting velocity (rpm) B	Amplitude of pole geometry (mm) C	Current (A) D	Working gap (mm) E	Finishing time (min) F	MRR(g) G	ΔSR (μm) H
1	6	200	6	4	3	16	0.0028	0.0401
2	10	700	45	4	2	20	0.0116	0.0812
3	10	700	12	6	1	16	0.0099	0.0776
4	6	1200	18	4	3	16	0.0176	0.0914
5	10	1200	12	2	2	16	0.0157	0.0784
6	10	200	12	2	2	16	0.0041	0.0590
7	6	700	6	6	2	12	0.0067	0.0576
8	10	1200	12	6	2	16	0.0159	0.0696
9	10	700	18	4	2	12	0.0128	0.0836
0	6	200	18	4	3	16	0.0053	0.0821
11	2	700	12	6	1	16	0.0104	0.0826
12	2	200	12	2	2	16	0.0039	0.0588
13	2	700	12	2	3	16	0.0092	0.0769
14	2	700	12	6	3	16	0.0090	0.0862
15	6	200	12	4	1	12	0.0043	0.0758
16	6	700	12	4	2	16	0.0099	0.0718
17	2	700	18	4	2	20	0.0121	0.0848
18	6	200	12	4	3	20	0.0042	0.0580
19	6	700	6	2	2	20	0.0067	0.0648
20	2	200	12	6	2	16	0.0044	0.0654
21	10	700	12	2	1	16	0.0105	0.0772
22	6	1200	6	4	1	16	0.0106	0.0549
23	10	200	12	6	2	16	0.0045	0.0649
24	10	700	12	2	3	16	0.0099	0.0822
25	10	700	6	4	2	20	0.0070	0.0690
26	6	700	6	6	2	20	0.0064	0.0685
27	6	200	12	4	1	20	0.0028	0.0678
28	6	700	18	2	2	20	0.0110	0.0992
29	6	200	12	4	3	12	0.0038	0.0573
30	6	1200	12	4	1	12	0.0147	0.0852
31	6	1200	12	4	3	20	0.0150	0.0844
32	6	700	12	4	2	16	0.0105	0.0680
33	6	700	18	6	2	12	0.0132	0.0746
34	2	700	6	4	2	12	0.0067	0.0498
35	6	700	18	6	2	20	0.0126	0.0746
36	6	700	18	2	2	12	0.0135	0.1092
37	6	200	6	4	1	16	0.0033	0.0560
38	10	700	6	4	2	12	0.0057	0.0708
39	6	1200	12	4	1	20	0.0133	0.1082
40	6	1200	6	4	3	16	0.0077	0.0534
41	6	700	12	4	2	16	0.0092	0.0909
42	10	700	12	6	3	16	0.0082	0.0944
43	6	700	12	4	2	16	0.0090	0.0865
44	6	700	12	4	2	16	0.0094	0.0868
45	6	1200	18	4	1	16	0.0188	0.1036
46	2	1200	12	2	2	16	0.0135	0.1026
47	2	700	18	4	2	12	0.0109	0.1064
48	6	1200	12	4	3	12	0.0104	0.1069
49	2	1200	12	6	2	1.5	0.0128	0.0974
50	6	700	12	4	2	16	0.0078	0.0668
51	6	700	6	2	2	12	0.0054	0.0654
52	2	700	6	4	2	20	0.0059	0.0662
53	6	200	18	4	1	16	0.0040	0.0704
54	2	700	12	2	1	16	0.0095	0.0872

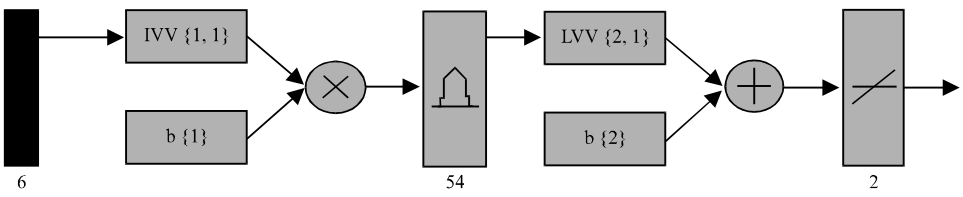

Fig. 1: Structure of RBFNN

Table 4: Results attained in RBFNN

Experiment MRR (g)	RBFNN MRR (g)	Error	Experiment SR (μm)	RBFNN SR (μm)	Error
0.0028	0.002670	0.046429	0.0401	0.043067	-0.07399
0.0116	0.010606	0.085690	0.0812	0.081333	-0.00164
0.0099	0.009508	0.039596	0.0776	0.077733	-0.00171
0.0176	0.017662	-0.003520	0.0914	0.091600	-0.00219
0.0157	0.015624	0.004841	0.0784	0.078533	-0.00170
0.0041	0.004566	-0.113660	0.0590	0.059333	-0.00564
0.0067	0.006714	-0.002090	0.0576	0.059333	-0.03009
0.0159	0.015932	-0.002010	0.0696	0.075600	-0.08621
0.0128	0.012896	-0.007500	0.0836	0.087467	-0.04626
0.0053	0.005310	-0.001890	0.0821	0.088933	-0.08323
0.0104	0.010416	-0.001540	0.0826	0.083067	-0.00565
0.0039	0.003588	0.080000	0.0588	0.059200	-0.00680
0.0092	0.008832	0.040000	0.0769	0.077200	-0.00390
0.0090	0.009028	-0.003110	0.0862	0.086267	-0.00078
0.0043	0.004368	-0.015810	0.0758	0.076000	-0.00264
0.0099	0.009342	0.056364	0.0718	0.078489	-0.09316
0.0121	0.012126	-0.002150	0.0848	0.086133	-0.01572
0.0042	0.004276	-0.018100	0.0580	0.062000	-0.06897
0.0067	0.007370	-0.100000	0.0648	0.066133	-0.02057
0.0044	0.004848	-0.101820	0.0654	0.066533	-0.01732
0.0105	0.010552	-0.004950	0.0772	0.078533	-0.01727
0.0106	0.010690	-0.008490	0.0549	0.056267	-0.02490
0.0045	0.004564	-0.014220	0.0649	0.066267	-0.02106
0.0099	0.009908	-0.000810	0.0822	0.083600	-0.01703
0.0070	0.006604	0.056571	0.0690	0.069733	-0.01062
0.0064	0.006100	0.046875	0.0685	0.072667	-0.06083
0.0028	0.002830	-0.010710	0.0678	0.074133	-0.09341
0.0110	0.011558	-0.050730	0.0992	0.099333	-0.00134
0.0038	0.004134	-0.087890	0.0573	0.057467	-0.00291
0.0147	0.014772	-0.004900	0.0852	0.085333	-0.00156
0.0150	0.015046	-0.003070	0.0844	0.084667	-0.00316
0.0105	0.009742	0.072190	0.0680	0.074489	-0.09543
0.0132	0.012696	0.038182	0.0746	0.074933	-0.00446
0.0067	0.006770	-0.010450	0.0498	0.050000	-0.00402
0.0126	0.012696	-0.007620	0.0746	0.074933	-0.00446
0.0135	0.013542	-0.003110	0.1092	0.110667	-0.01343
0.0033	0.003370	-0.021210	0.0560	0.056267	-0.00477
0.0057	0.005722	-0.003860	0.0708	0.071067	-0.00377
0.0133	0.013318	-0.001350	0.1082	0.109733	-0.01417
0.0077	0.007738	-0.004940	0.0534	0.056400	-0.05618
0.0092	0.009342	-0.015430	0.0909	0.085849	0.055567
0.0082	0.008290	-0.010980	0.0944	0.098400	-0.04237
0.0090	0.009342	-0.038000	0.0865	0.078489	0.092613
0.0094	0.009342	0.006170	0.0868	0.078489	0.095749
0.0188	0.019048	-0.013190	0.1036	0.101600	0.019305
0.0135	0.013542	-0.003110	0.1026	0.103200	-0.00585
0.0109	0.010978	-0.007160	0.1064	0.106533	-0.00125
0.0104	0.010416	-0.001540	0.1069	0.111200	-0.04022
0.0128	0.012896	-0.007500	0.0974	0.098000	-0.00616
0.0078	0.008542	-0.095130	0.0668	0.071823	-0.07519
0.0054	0.005490	-0.016670	0.0654	0.066400	-0.01529
0.0059	0.005974	-0.012540	0.0662	0.066533	-0.00503
0.0040	0.004082	-0.020500	0.0704	0.071467	-0.01516
0.0095	0.009558	-0.00611	0.0872	0.087333	-0.00153

function in radial base occur. The normalized Gaussian function usually utilized as the RBF, i.e.:

$$\varphi_i(x) = \exp\left(\frac{\left\|x-\mu^2\right\|}{2\sigma_i^2}\right) \quad (2)$$

where, μ_i and σ_i denote center of the ith node and the spread width, respectively. Normally, the RBFNN training is classified into two stages: compute the parameters of RBFs, i.e., spread Gaussian center and width. In normal, k-means clustering methodology was usually utilized here. Assess the output weight by observing, learning methodology. Usually Recursive Least Square (RLS) and Least Mean Square (LMS) were utilized.

The primary phase is highly complex because the location and number of centres in the hidden layer force fully affect the performance of the RBFNN. The predicted values acquired out of RBFNN are not convinced, the amount of the response (MRR and SR) are high compare with the experimental value as in Table 4, therefore, an error is also high. So, ANN is carried out to determine the predicted values.

Back propagation neural network: ANN consists of three layers, the first layer is called an input layer, single or more of hidden (unobserved) layers are the second layer finally, the third layer is called the output layer. Not only the output but also, the hidden layers have processing elements and interconnections called synapses and neurons correspondingly. Each interconnection link with connection weight or strength. Very carefully decided the hidden layers and nodes of each layer, since, if the system has too little hidden layer units, it cannot model the specific information. However, many of these units determine the capability of the network to popularize the results for this reason, the resulting model would not work completely for novel incoming data. Each processing element primarily achieves a weighted accumulation of the corresponding input values and then the result is passed through an activation function. Since, there is no calculation was performing in the input layer node, the overall input to each node is the mean weighted output of the nodes in the first layer.

Proposed ANN Model: As shown in Fig. 2 and 3, the design of feed forward which contains multi-layers network by the algorithm of back propagation learning is (6-20-2) for MAF. The training of NN contains two passes are forward pass and reverse pass, propagation of input signals to output from within the network called forward pass while propagation of the determined error signals back out of the network called reverse pass where they are utilized in adjust the values of the weights.

Two models, namely, the RBFNN and ANN are built and estimated. The ANN back propagation technique with an estimated of predictive model gives kindly result compared to RBFNN Model with values close to the experimental results as shown in Table 5.

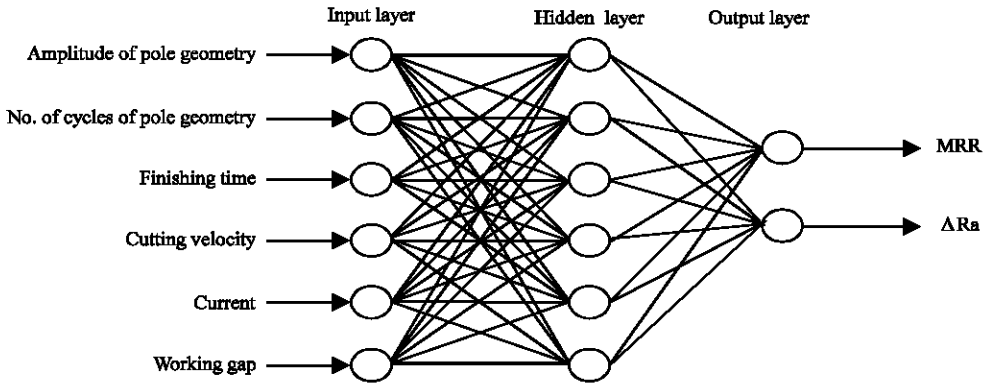

Fig. 2: Neural network Model

Table 5: Results obtained from artificial neural network

Experiment MRR (g)	ANN MRR	Error (%)	Experiment SR (μm)	ANN SR (μm)	Error (%)
0.0028	0.002972	-0.061430	0.0401	0.040959	-0.02142
0.0116	0.010933	0.057500	0.0812	0.079641	0.01920
0.0099	0.010199	-0.030200	0.0776	0.078059	-0.00591
0.0176	0.017195	0.023011	0.0914	0.090840	0.006127
0.0157	0.014663	0.066051	0.0784	0.078683	-0.00361
0.0041	0.003808	0.071220	0.0590	0.060373	-0.02327
0.0067	0.006759	-0.008810	0.0576	0.058053	-0.00786
0.0159	0.017658	-0.110570	0.0696	0.074395	-0.06889
0.0128	0.012387	0.032266	0.0836	0.084015	-0.00496
0.0053	0.005615	-0.059430	0.0821	0.082977	-0.01068
0.0104	0.010689	-0.027790	0.0826	0.081541	0.012821
0.0039	0.003962	-0.015900	0.0588	0.058764	0.000612
0.0092	0.009518	-0.034570	0.0769	0.083212	-0.08208
0.0090	0.008439	0.062333	0.0862	0.084736	0.016984
0.0043	0.004372	-0.016740	0.0758	0.076751	-0.01255
0.0099	0.009004	0.090505	0.0718	0.078531	-0.09375
0.0121	0.013415	-0.108680	0.0848	0.110649	-0.30482
0.0042	0.004168	0.007619	0.0580	0.057633	0.006328
0.0067	0.005168	0.228657	0.0648	0.059755	0.077855
0.0044	0.004744	-0.078180	0.0654	0.065212	0.002875
0.0105	0.008625	0.178571	0.0772	0.056131	0.272915
0.0106	0.010757	-0.014810	0.0549	0.055299	-0.00727
0.0045	0.004772	-0.060440	0.0649	0.065089	-0.00291
0.0099	0.008840	0.107071	0.0822	0.082773	-0.00697
0.0070	0.006889	0.015857	0.0690	0.089683	-0.29975

Table 5: Continue

Experiment MRR (g)	ANN MRR	Error (%)	Experiment SR (μm)	ANN SR (μm)	Error (%)
0.0064	0.006414	-0.002190	0.0685	0.067133	0.019956
0.0028	0.003876	-0.384290	0.0678	0.069156	-0.02000
0.0110	0.009535	0.133182	0.0992	0.099304	-0.00105
0.0038	0.005466	-0.438420	0.0573	0.061305	-0.06990
0.0147	0.014434	0.018095	0.0852	0.085308	-0.00127
0.0150	0.014644	0.023733	0.0844	0.083771	0.007453
0.0105	0.009004	0.142476	0.0680	0.078531	-0.15487
0.0132	0.012312	0.067273	0.0746	0.075716	-0.01496
0.0067	0.007176	-0.071040	0.0498	0.050464	-0.01333
0.0126	0.011369	0.097698	0.0746	0.073227	0.018405
0.0135	0.014102	-0.044590	0.1092	0.104684	0.041355
0.0033	0.003348	-0.014550	0.0560	0.056887	-0.01584
0.0057	0.005936	-0.041400	0.0708	0.073987	-0.04501
0.0133	0.013587	-0.021580	0.1082	0.108492	-0.00270
0.0077	0.007774	-0.009610	0.0534	0.052692	0.013258
0.0092	0.009004	0.021304	0.0909	0.078531	0.136073
0.0082	0.008406	-0.025120	0.0944	0.093960	0.004661
0.0090	0.009004	-0.000440	0.0865	0.078531	0.092127
0.0094	0.009004	0.042128	0.0868	0.078531	0.095265
0.0188	0.021110	-0.122870	0.1036	0.100492	0.03000
0.0135	0.012417	0.080222	0.1026	0.102289	0.003031
0.0109	0.010850	0.004587	0.1064	0.106657	-0.00242
0.0104	0.010228	0.016538	0.1069	0.107537	-0.00596
0.0128	0.012237	0.043984	0.0974	0.093837	0.036581
0.0078	0.009004	-0.154360	0.0668	0.078531	-0.17561
0.0054	0.005495	-0.017590	0.0654	0.065497	-0.00148
0.0059	0.006114	-0.036270	0.0662	0.065300	0.013595
0.0040	0.003695	0.076250	0.0704	0.063152	0.102955
0.0095	0.009558	-0.006110	0.0872	0.087092	0.001239

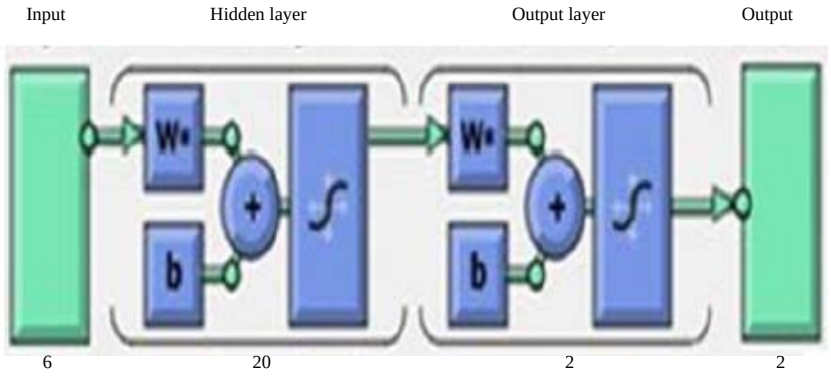

Fig. 3: Proposed NN architecture for MAF

RESULTS AND DISCUSSION

The Model of RBFNN and ANN that proposed to predict the MRR gave a result of output that nearly closer to the targets with correlation (0.955174) for the RBFNN and (0.965254) for ANN while the SR with correlation (0.931547) for the RBFNN and (0.942041) for ANN. The line chart for MRR and SR are shown in Fig. 4 and 5 along with the different input parameters by RBFNN and ANN. The error percentage for MRR is around between (-0.11366) minimum and (0.08569) maximum for RBFNN, (-0.06143) minimum and (0.02286) maximum for ANN. MRR correlates with the cutting velocity and amplitude of pole geometry. Whereas the error percentage for SR (-0.09543) minimum and (0.095749) maximum for RBFNN, (-0.02142) minimum and (0.02729) maximum for ANN. SR correlates with the input parameters working gap and current.

The ANN is the greatest tool for the predictive values of AISI 316 SS by MAF. Here, MRR leads to increase, noticeably showing a rise in cutting velocity for any specified value of the amplitude of pole geometry perfect instance. Thus, maximum MRR is received at an amplitude of pole geometry and cutting velocity (Fig. 6). High temperature of work piece produces with the increase in cutting velocity that grounds many materials. The SR

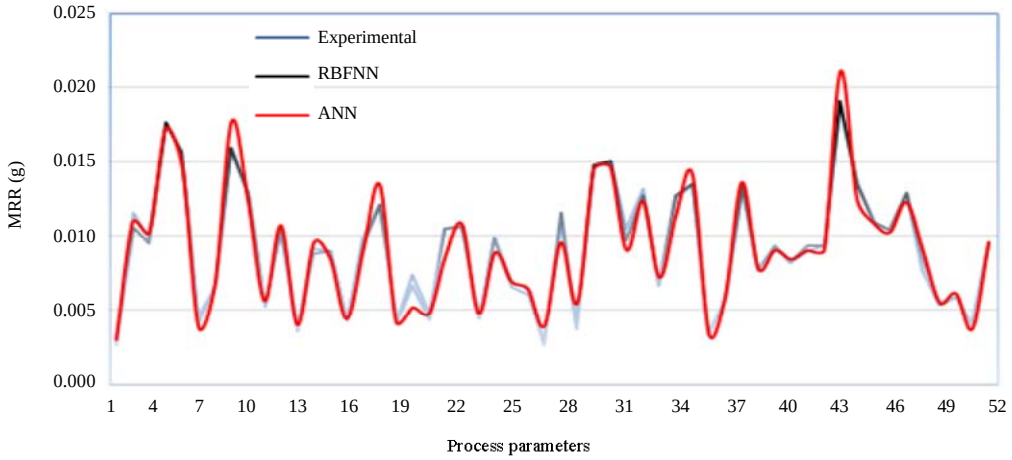

Fig. 4: Line chart of MRR for AISI 316 SS

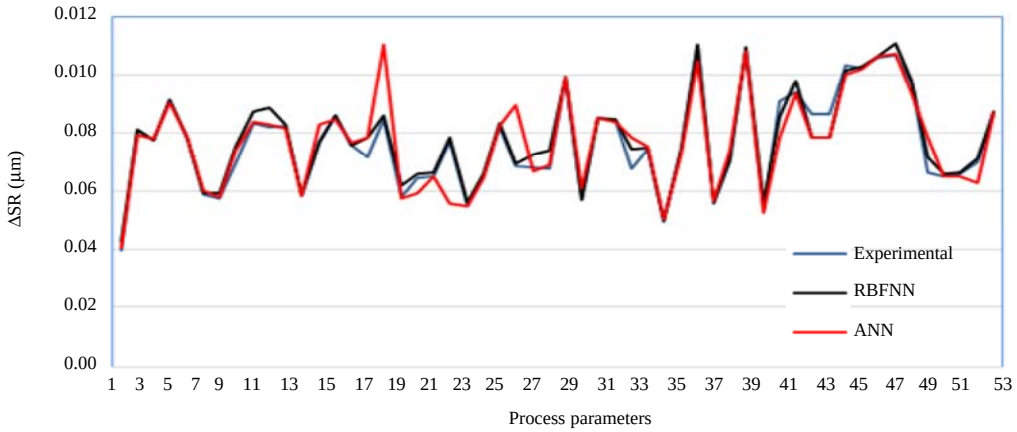

Fig. 5: Line chart of SR for AISI 316 SS

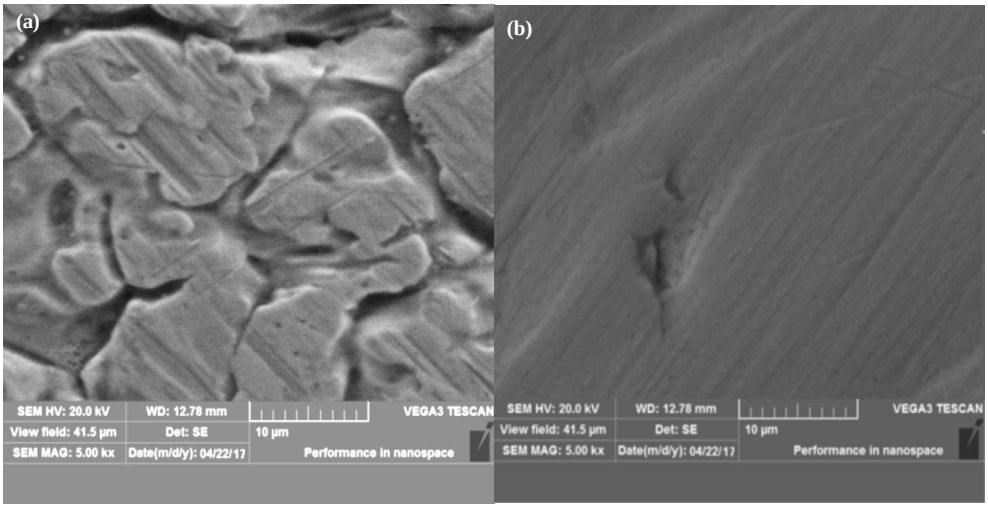

Fig. 6: SEM snap of AISI 316 SS at condition: a) SEM snap at condition: A = 2, B = 700, C = 12, D = 2, E = 1, F = 16, SR= 0.0872 μm; b) SEM snap at condition: A = 2, B = 700, C = 12, D = 6, E = 3, F = 16, SR = 0.0862 μm

value decreases with the increase of working gap and current while keeping the other factors constant at their middle levels, more specifically can decrease from 0.0872-0.0862 μm as shown in Fig. 6.

CONCLUSION

The prediction of MAF response parameters is made by conducting experiments on AISI 316 SS using RBFNN and ANN. Various levels of input process parameters have been taken into consideration depending on the Box Behnken design of MAF machine to carry out the experiments. In order to predict the object, RBFNN and ANN Models have been built with the aid of experimental results. Depending on the above two methods, it is concluded that the maximum error attained in RBFNN Model is 0.08569 and in ANN Model is 0.02286 for MRR whereas for SR is 0.095749 and 0.02729 in RBFNN and ANN, respectively. Eventually, it is evidenced that the network's model created using ANN's gives optimum values compared to RBFNN Model.

REFERENCES

Bang-Zhong, L. and Z. Jin-Jin, 2005. Research on surface characteristics of non-traditional finishing. J. Zhejiang Univ. Sci. A., 6: 1152-1157.

Chang, G.W., B.H. Yan and R.T. Hsu, 2002. Study on cylindrical magnetic abrasive finishing using unbounded magnetic abrasives. Int. J. Mach. Tools Manuf., 42: 575-583.

Jain, V.K., P. Kumar, P.K. Behra and S.C. Jayswal, 2001. Effect of working gap and circumferential speed on the performance of magnetic abrasive finishing process. Wear, 250: 384-390.

Jayakumar, P., 2001. Semi magnetic abrasive machining. Proceedings of the 4th International Conference on Mechanical Engineering (ICME'01), December 26-28, 2001, Bangladesh University of Engineering and Technology, Dhaka, Bangladesh, pp: 81-85.

Khairy, A.B., 2001. Aspects of surface and edge finish by magnetoabrasive particles. J. Mater. Process. Technol., 116: 77-83.

Kwak, J.S. and C.M. Shin, 2011. Parameter optimization and development of prediction model for second generation magnetic abrasive polishing of AZ31B plate. Proceedings of the International MultiConference on Engineers and Computer Scientists (IMECS'11) Vol. 2, March 16-18, 2011, International Association of Engineers (IAENG), Hong Kong, ISBN:978-988-19251-2-1, pp: 1-7.

Raghuram, M.G.V.S. and S.S. Joshi, 2008. Modeling of polishing mechanism in magnetic abrasive polishing. Proceedings of the 12th International Conference on International Association for Computer Methods and Advances in Geomechanics (IACMAG'08), October 1-6, 2008, IACMAG, Goa, India, pp: 344-352.

Singh, A.K., S. Jha and P.M. Pandey, 2010. Nanofinishing Process for 3D Freeform Surfaces Using Ball End MR Finishing Tool. In: Proceedings of the 36th International MATADOR Conference, Singh, A.K., S. Jha and P.M. Pandey (Eds.). Springer, London, England, UK., ISBN:978-1-84996-431-9, pp: 67-70.

Yamaguchi, H. and T. Shinmura, 1999. Study of the surface modification resulting from an internal magnetic abrasive finishing process. Wear, 225: 246-255.

Yamaguchi, H. and T. Shinmura, 2000. Study of an internal magnetic abrasive finishing using a pole rotation system: Discussion of the characteristic abrasive behavior. Precis. Eng., 24: 237-244.